

Mechanical and Energy Engineering

**Outdoor Testing of a Zig-Zag Solar Air heater with and without
Artificial Roughness on Absorber Plate**

Dr. Mahmoud Maustafa Mahdi*

Lecturer

Electromechanical Eng –University of Technology

Email: Mahmoud_mahdi74@yahoo.com

Dr. Ameer Abed Gaddoa

Lecturer

Electromechanical Eng. –University of Technology

Email: en_ameerabed@yahoo.com

ABSTRACT

In this paper, thermal performance of a zig-zag solar air heater (ZZSAH) with and without using steel wire mesh on the absorber plate of the collector is experimentally investigated. The experimental work includes four inclination angles of the collector 20°, 30°, 45°, and 60° and four air mass flow rates of 0.03, 0.04, 0.06, and 0.08 kg/s under varieties of operating conditions of a geographic location of Baghdad. New correlation equations of Nusselt number are obtained from experimental results for both types of collectors where the effect of varying of the inclination angle of collector taken into consideration in the experiment. The correlations show good agreement with the present experimental data. In addition, the effects of mass flow rate and temperature rise across the efficiency of collector air heater are investigated. The results reveal that the efficiency of (ZZSAH) at 45° inclination angle reaches the highest values among other degrees of inclination angles for both types of collectors under study. The results also show that the addition of wire mesh magnifies the effect of inclination angle.

Keywords: outdoor testing, solar air heater, experimental correlation.

**الأختبار عند الظروف الخارجية لمنظومة سخان الهواء الشمسي ذات المجرى الهوائي المتعرج مع وبدون
خشونة صناعية على السطح الأمتصاصي للسخان**

د. امير عبد جدوع

مدرس

الهندسة الكهروميكانيكية- الجامعة التكنولوجية

د. محمود مصطفى مهدي

مدرس

الهندسة الكهروميكانيكية- الجامعة التكنولوجية

الخلاصة

نفذت دراسة عملية لتحليل الأداء الحراري لمنظومة سخان الهواء الشمسي ذات المجرى الهوائي المتعرج مع وبدون استخدام خشونة صناعية بالإضافة قماش معدني فولاذي على لوح سطح الامتصاص لمجمع شمسي. شملت الدراسة العملية اربع زوايا ميل للمجمع الشمسي وهي 20، 30، 45، و 60 درجة، ومعدلات تدفق الهواء وهي 0.03، 0.04، 0.06 و 0.08 كيلوغرام/ ثانية وذلك تحت ظروف تشغيلية مختلفة عند الموقع الجغرافي لمدينة بغداد. استحدثت معادلات تجريبية، لعدد نسلت، ربطت بين

*Corresponding author

Peer review under the responsibility of University of Baghdad.

<https://doi.org/10.31026/j.eng.2019.04.01>

2520-3339 © 2019 University of Baghdad. Production and hosting by Journal of Engineering.

This is an open access article under the CC BY-NC license <http://creativecommons.org/licenses/by-nc/4.0/>.

Article received: 22/1/2018

Article accepted: 9/5/2018



الظروف التشغيلية والتصميمية وذلك لنوعين من المجمعات مع وبدون استخدام قماش معدني وادخل في المعادلات التجريبية تأثير زاوية ميل المجمع الشمسي. وظهرت هذه المعادلات التجريبية اتفاقا جيدا مع البيانات والنتائج التجريبية. وبالإضافة الى ماتقدم تم التحقق من تأثير كل من معدل التدفق الكتلي للهواء وارتفاع درجة حرارة الهواء غير المجمع على كفاءة المجمع ومتوسط معامل انتقال الحرارة للمجمع. كشفت النتائج على ان كفاءة المجمع الهواء الشمسي يكون له اعلى قيمة عند زاوية ميل 45 درجة وذلك لكلا النوعين مع وبدون قماش معدني. وظهرت النتائج أيضا ان أضافه القماش المعدني الخشن على السطح الامتصاصي للمجمع يعمل على تضخيم تأثير زاوية ميل المجمع الهوائي الشمسي.

1- INTRODUCTION

Flat plate collectors can be either gas collector or water collector based on the used fluid, in the collector. The efficiency of solar air heaters is naturally low because the air has bad thermodynamic properties in terms of heat transfer characteristics in comparison with liquid. Therefore, many studies have been provided to improve the thermal performance of the collector for multi types of solar air heaters.

Solar air heaters utilize solar energy to heat the air as a simple device. Recently, the solar air heaters have been employed in many application which requires low to moderate temperature below 70 °C such as space heating and products drying.

Many studies have been conducted recently, on the energy analysis and the thermal performance of the solar air heater. A friction similarity law and a heat transfer analogy were developed by **Dippery and Saberskey 1963**. **Han, et al., 1978**, investigated the effect of rib shape, pitch to rib height ratio (p/e) and angle of attaching of the rib. The effect of rib orientation on local heat transfer and pressure drop was investigated by **Han, et al., 1991**. They found that the maximum value of the heat transfer coefficient occurs at a relative roughness pitch of 10.

Gupta, et al., 1997, proposed the effect of rib roughness on fluid flow and heat transfer in rectangular passages with only one heated surface having artificial rib roughness. **Gupta et al. 1997** developed a relationship between the solar air heater system and operating parameters where the correlation based on the low of wall similarity and heat moment transfer analogy.

Prasad and Saini 1998, determined numerically the heat transfer and flow friction in a square duct with discrete ribs. They suggested that, at dawn stream of the rib, the heat transfer was augmented exteremly because of strong secondary. A rectangular duct solar air heater with absorber plate that having V-shaped ribs was investigated by **Momin, et al., 2002**. They pointed out that the V-shaped rib arrangement can yield better performance in comparison with continuous rib arrangement.

The effect of the geometrical parameter on the heat transfer and fluid flow characteristics was presented by **Forson, et al., 2003**. **Tasuni, et al., 2003**, investigated numerically the heat transfer and flow friction in a square duct with discrete ribs. They found that, at dawn stream of the rib, the heat transfer was increased considerably because of strong secondary flow.

Chaube, et al., 2006, determined the turbulent flow behaviors using the (k-w) turbulent model in a two dimensional roughed channel with heating from one side only. **Promvong and Thianpony, 2008**, experimentally studied the thermal behaviors for using wedge- ribs, triangular and rectangular ribs on the two opposite duct wells. They claimed that the maximum heat transfer is seen at wedge rib pointing downstream.



Eiamsaard and Promvonge, 2008, analyzed the 2D flow resistance and heat transfer in a periodic groove channel. They found out that the using of grooved channel results in the increasing of the heat transfer about 158% higher than the smooth channel. **Anil and Bhagoria, 2013**, investigated numerically the heat transfer and fluid flow characteristics of fully developed turbulent flow in a rectangular duct having repeated transverse square sectioned rib roughness on the absorber plate. They found that the square sectioned transverse rib roughened duct with $P/e=10.71$ and $e/d=0.042$ resulted in the best thermo-hydraulic performance parameter for the considered range of parameter. **Anil and Bhagori 2014**, studied the heat transfer and fluid flow processes in an artificially roughened solar air heater by using computational fluid dynamic (CFD). The result of their study shows that the Nusselt number and average friction factor increase in relative roughness pitch. The condition for optimum performance has been determined in term of thermal enhancements factor. **Skullong, 2017**, determined the influence of inclined ribs (mounted on the absorber) on the thermal performance of a solar air heater duct and it was claimed that the rib artificial roughness is a promising method for the performance improvement of a solar thermal system. **Sanjay, et al., 2017**, investigated experimentally and numerically the heat transfer characteristic of a solar air heater with ribs. The results showed that the rib placement on the absorber plate effects on the heat transfer and fluid flow characteristic.

According to the literature, it can be claimed that there is no study has been carried out on the zig-zag solar air heater to study the effect of the inclination angle of the solar collector and location of the optimum inclination angle of this type. In this study, the efficiency of a solar air heater with and without wire mesh on absorber plate is experimentally investigated. Furthermore, new correlation equations including dimensionless group Nusselt number, Reynolds number, and effect of the inclination angle of the collector for the two types with and without wire mesh are obtained from the experiments.

2. EXPERIMENTAL SETUP AND MEASUREMENT

An experimental work on a Zig-Zag solar air heater with and without metal wire mesh was conducted at the geographic location of Baghdad. A schematic diagram of the experimental setup is shown in **Fig. 1a** the two collectors designed are composed of basically the same materials and dimensions as a flat plate solar air heater. One of them has a metal wire mesh on the absorber surface. The absorber plates are formed by a black painted galvanized with 0.6 mm thick. In order to let the air pass through the collector space in a wider channel, a baffle was mounted and soldered on the absorber plate along a Zig-Zag, flow path as shown in **Fig. 1a**.

The baffles were made of the galvanized sheet with a thickness of 2mm. The two collectors have (120 cm × 80 cm) dimension. The frame of the solar collector was made of wood and covered with Aluminum. A single normal window glazing of 0.4 cm thickness was chosen to increase the radiation impact on the absorber surface. The side and the bottom of the case frame were insulated with 5 cm thick glass wool in order to minimize heat losses from the bottom and from the sides of the collector.

A steel wire mesh (0.1×0.1 cm), **Fig.1b**, cross-section opening with 0.025 cm in diameter was fixed on the absorber plate in the type of solar air heater with metal wire mesh. The air was provided by a centrifugal blower through the pipe and control regulator was used to change the air volume flow rate. In order to record the temperature at different hours of the day. A (T type thermocouples) were



used to measure the temperatures at the inlet and outlet of the collector. A (T type thermocouples) were used at different places. Ambient temperature was measured by the thermocouple placed under the collector. The collector was faced toward south and its tilt angle was varied from 20° to 60°.

The experiment was carried out in August and September. Both collectors were located to south direction. The tests were started at 8 Am and finished at 6 pm of the day for various mass flow rate and four inclination angles and performed 2 days for each flow rate and tilt angle. In order to perform a fair comparison between the mentioned collectors, the tests have been carried on approximately the same radiation intensity days.

An electrical blower has been used to supply the air flow rate through the collector and the air flow rate was adjusted via a regulator valve located at the blower outlet. In both collectors the air flow rate was kept constant and the same. Four air mass flow rate was adjusted and measured by using ratio meters and four inclination angles were varied for each mass flow rate. The inclination angles were adjusted via sliding protractors.

A Pyranometer was used to measure the incident solar digital radiation. T-type thermocouples were placed at the inlet and outlet of the airports as well as six points in the solar collector. All thermocouples wire were connected to a digital thermometer through compensating leads and a multi-channel selector switch.

3. RESULTS AND DISCUSSION

Two type of solar air heaters have been tested outdoor. The first one was without wire mesh and the second was with wire mesh on the absorber. Each test included four air mass flow rate at various tilt angles. Solar radiation, temperature and air flow rate have been measured. Moreover, the effect of using wire mesh on the temperature rise across the collector and collector efficiency was investigated.

A comparison has been carried out between the collectors under study in terms of efficiency as well as temperature rise. Seeking a fair comparison, the experiment tests for both collectors were carried out on the same day. The effect of the various operating factors on the performance of the two types of solar air heater will be discussed in the following sections.

The following expression for the instantaneous thermal efficiency of the solar air heater has been used in the present analysis:

$$\eta_{ins} = \frac{\text{useful heat gain}}{\text{incident solar radiation}}$$

$$\eta_{ins} = \frac{Q_u}{IA_c} \quad (1)$$

$$Q_u = \dot{m}cp(T_{fo} - T_{fi}) \quad (2)$$

Ac = surface area of the collector plate, m².

I= irradiance, W/m².



3.1 The effect of air flow rate

The impact of varying air mass flow rates on the temperature rise across the collector is presented in **Fig. 2** and **Fig. 3**. These figures show that the temperature rise decrease with increasing mass flow rate for both collectors where the maximum temperature rise across the collector is 14 °C at 14 PM for the roughened collector with wire mesh, while the temperature rise is 11°C at 14 PM for the collector without wire mesh as shown in **Fig. 3**. For both types, the temperature rise is obtained at the minimum air flow rate of 0.03 Kg/s and the inclination angle of 45°.

Fig. 4 and **Fig. 5** show the hourly efficiency of the collector per typical day at a different air mass flow rate and 45° inclination angle. It can be seen from the figures that the efficiency increases and reaches to a peak value at 14 PM then it decreases slightly until 18 pm. It can be observed also that the efficiency behavior curve does not follow the solar radiation intensity curve shown in **Fig.6**. This is due to the stored energy in the wire mesh layer.

Varying the instantaneous efficiency (η_{ins}) with the air mass flow rate for different inclination angle is shown in **Fig.7** and **Fig. 8**. It can be shown obviously that the efficiency increases with increasing of the flow rate for different inclination angles for both collectors. In addition, the maximum efficiencies for both collectors are 57% and 42 % respectively as shown in **Fig.7** and **Fig.8**.

It can be noticed from the aforementioned discussion that the using wire mesh on the absorber plate improves the efficiency. This is because of increasing the heat transfer coefficient which gives higher outlet air temperature.

3.2 The effect of the inclination angle

The variation of the temperature rise across the collector is analyzed by considering four inclination angles varying from 20° to 60° and different air mass flow rate. Generally, the inclination orientation of ($\alpha = 45^\circ$) shows a considerable increase in temperature when compared with the temperature rise across the collector of the other inclination angles for all air mass flow rate values and for both types of collectors. **Fig.9** shows the temperature rise with the air mass flow rate for various inclination angles for the collector without wire mesh. It can be observed that the effect of inclination angle is not really significant in the range ($\alpha=20^\circ$ to $\alpha=60^\circ$) at low air mass flow rates of (0.03 kg/s) where the temperature rises across the collector was less than (0.75 °C) for various inclination angle.

In addition, the results show that the increase of the air mass flow leads to increase the sensitivity of collector to the variation of inclination angle, where the temperature rise across the collector was more than 2.5 °C at a high mass flow rate of (0.08kg/s). **Fig.10** shows that the effect of air mass flow rate on the temperature rise across the collector at 12 pm for four inclination angles for a wire mesh collector. It also can be seen that the behavior of the temperature rise for both types of collectores is quiet similar to **Fig.11**, depicts the variation of the temperature rise across the collector with the air mass flow rate for both type of collectors at 12 pm and for 45° inclination angle.

Further, the results reveal that an inclination angle ($\alpha = 45^\circ$), the temperature rise across wire mesh the collector is more sensitive to the air mass flow rate than the collector without wire mesh, where the temperature rise at across the wire mesh collector is 13.5 °C at 12 PM, while for the one without wire mesh collector is 10°C. This effect is better portraged in **Fig.12**, for the same inclination angle.



It is clear from the aforementioned discussion that the using a wire mesh magnify the impact of inclination angle and the use of a wire mesh collector increase the temperature rise across the collector as a result of considerable improvement in the heat transfer coefficient.

3.3 Factors affecting the heat transfer coefficient

It was pointed out that the supplying high values of solar radiation to the inclined collector surface, heat will be transported to the air passing through the wire mesh by forced convection. In this case, the heat transfer will be from the wire mesh. This phenomenon depends strongly on the amount of the air mass flow rate and the inclination angle. **Figs. 13 and 14** show the effects of the air mass flow rate on the heat transfer coefficient for various inclination angles for both types of considered collectors at 12 PM. It can be seen from these figures that the heat transfer coefficient increases slightly with air mass flow rate, particularly at a high air mass flow rate.

This is due to a more active motion of air where this leads to decrease the thermal resistance at the surface of collector. It can be observed also that the heat transfer coefficient of the collector with a wire mesh is larger than the collector without wire mesh at all inclination angles. Besides the heat transfer coefficient of the collector with wire mesh is about 50% higher than the one without wire mesh at an inclination angle of 45°. This is due to the high solar radiation intensity incident on the collector and minimum temperature difference between the roughened plate and the air passing over the mesh. **Fig.14** indicates the optimum angle of inclination is 45° because the heat transfer coefficient reaches the maximum value at this angle. **Fig.15** depicts the effect of solar intensity on the heat transfer coefficient for wire mesh collector with various air mass flow rates and for 45° inclination angle.

This figure shows that the heat transfer coefficient is improved considerably with increasing of the solar intensity for all air mass flow rates. **Fig.16** shows the influence of the air mass flow rate on the heat transfer coefficient for both types of collector under study.

This figure shows that the heat transfer coefficient for the collector without wire mesh increases slightly with air mass flow rate, whereas the heat transfer coefficient for the collector with a wire mesh shows a better improvement with air mass flow rate. This means the air mass flow affects the collector with wire mesh more considerably than the collector without wire mesh.

It can be concluded that the improvement of the heat transfer coefficient with using the wire mesh is much better than without using wire mesh flow.

3.4 Correlation for Nusselt Number

Mechanism and nature studying of the heat transfer coefficient depends on the level of the heat flux that depends on the temperature difference and other parameters. It has been shown that Nusselt Number (Nu) is a function of dimensional parameters Reynolds Number (Re).

$$Nu = f(Re) \quad (3)$$

$$Re = \frac{v D_h}{\vartheta_{air}} \quad (4)$$

Where:

ϑ_{air} = Kinematic viscosity of air at t_{av} in m^2/sec .



$D_h = 4 \times \text{Area of cross section/perimeter.}$

$$D_h = 4WH/2(W + H)$$

$v = \text{velocity of the air.}$

$$v = \dot{m}/\rho WH.$$

$\dot{m} = \text{mass flow rate, } \frac{\text{kg}}{\text{s}}.$

$\rho = \text{density of air, Kg/m}^3.$

$H = \text{height of the air passage.}$

$W = \text{width of air passage.}$

$$Nu = \frac{h_{cal} \cdot D_h}{K_{air}} \quad (5)$$

$D_h = \text{is hydraulic mean diameter based on entire wetted parameter.}$

$h_{cal} = \text{calculated heat transfer coefficient.}$

$K_{air} = \text{is thermal conductivity of air.}$

$$h_{cal} = \frac{Q_u}{A \cdot (T_{pm} - T_{fm})} \quad (6)$$

Where:

$Q_u = \text{useful heat gain of the air, equation (2).}$

$C_p = \text{is spesific heat of air.}$

$T_{fo} = \text{is air temperature at exit of collector.}$

$T_{fi} = \text{is air temperature at inlet to the collector.}$

$T_{pm} = \text{is the average value of the heater sur}$

$\text{face temperature(average plate temperature).}$



$$T_{pm} = (T_{p1} + T_{p2} + T_{p3} + T_{p4} + T_{p5})/5 \quad (7)$$

$T_{p1}, T_{p2}, T_{p3}, T_{p4}, T_{p5}$ = local plate temperature , °C.

T_{fm} = is the average air temperature in the solar air heater

$$T_{fm} = (T_{fi} - T_{fo})/2$$

It can be noted that these relations are valid for the certain constant inclination angle of the solar air heater. It has been revealed that the heat transfer mechanism can be enhanced by utilizing wire mesh on the absorber plate of the solar air heater. In this study, a new correlation to predict the average Nusselt number is developed by considering the wire mesh on the absorber plate. The change in inclination angle of the solar air heater affects the solar radiation which reaches the absorber plate as well as the flow of the air passing the absorber plate, i.e. the heat transfer mechanism will be affected. In order to describe the contribution of the solar air heater orientation to the heat transfer process, equation (8) has been suggested by **Nguyenchi and Groll, 1982**, Thereby, relation (3) is modified to include the effect of the mentioned parameter as shown in equation (9).

$$F_A = f(\alpha) = \frac{\alpha}{180} + \sqrt{\sin 2\alpha} \quad (8)$$

$$Nu = f(Re, F_A) \quad (9)$$

A possible form of the above equation is a power law which is useful in many heat transfer problems, in the form:

$$Nu = A_o Re^{a_o} F_A^{b_o} \quad (10)$$

It is worth mentioning that F_A , Re , and Nu are directly calculated from equations (8), (4) and (5), to derive a correlation for the experimental results. A statistical correlation has been developed based on regression analysis and experimental data. A log-log plot of the Nusselt number as a function of F_A (the function of angle) for a smooth and roughed surface of a solar air heater is shown in **Fig.17** from which and from data point obtained relating the average Nusselt number and the function of inclination angle F_A as :

$$Nu = A_o (F_A)^0 \quad (11)$$

For solar air heater without mesh. By taking the Reynolds number into consideration the value:

$$(Nu)/F_A^{0.25} = A_o \quad (12)$$

are plotted on a log-log against Reynolds number as shown in **Fig.18** for the case of solar air heater without mesh a straight line (depending on regression analysis) on a log-log scale yields :

$$(Nu/F_A^{0.25}) = 0.241 Re^{0.541} \quad (13)$$



For the solar air heater without mesh. The final correlation is :

$$Nu_{corr} = 0.241Re^{0.541}F_A^{0.25} \quad (14)$$

For solar air heater without mesh the heat transfer coefficient, h_{corr} can be determined by:

$$h_{corr} = Nu_{corr} \cdot K_{air} / D_h \quad (15)$$

This value is shown in **Fig.19** which is in agreement with the most of data for solar air heater without mesh to within $\pm 7\%$. The same procedure has been followed (depending on regression analysis) to correlate data for solar air heat with mesh. The final term of the correlation is:

$$Nu_{corr} = 0.151Re^{0.651}F_A^{0.21} \quad (16)$$

The data of the heat transfer coefficient h_{corr} is fit within $\pm 6\%$ as shown in **Fig.20**.

4. CONCLUSIONS

An experimental investigation is conducted on a zig-zag solar air heater with and without wire mesh to analyze their thermal performance under four different inclination angles and flow rates values. It can be concluded that the solar air heater with a wire mesh is more sensitive to the variation in inclination angle than the one without mesh, particularly at a low air mass flow rate. Besides the heat transfer coefficient is found to be a strong function of the air mass flow rate especially in the solar air heater with a wire mesh. In addition, it is found that in order to obtain a high heat transfer coefficient and for a high air mass flow rate, it is necessary to orient the solar air heater at a 45° angle. Further, the solar air heater with a wire mesh shows a significant effect of the air mass flow rate on the temperature rise across the collector at an inclination angle of 45° when comparing with collector without wire mesh. Furthermore, solar air heater with a wire mesh operates at higher instantaneous efficiency than air heater without wire mesh for all operating conditions that is mean, the performance of the solar air heater with wire mesh was more significant in term of heat transfer coefficient than that without wire mesh.

5. REFERENCES

- Anil Singh Yadar, and J.L.Bhagoria 2014, a numerical investigation of square sectioned transverse rib roughened solar air heater, International Journal of Thermal Science, Vol. 79, PP.111-131.
- Anil Singh Yadar, and J.L.Bhagoria 2013, A CFD based heat transfer and fluid flow analysis of a solar air heater provided with circular transverse wire rib roughness on the absorber plate. Energy, Vol. 35, PP.1127-1142.



- Chaube A, Sahoo, P.K. and Solanki, S.C.2006, Analysis of heat augmentation and flow characteristics duct due to rib roughness over absorber plate of a solar air heater. Renewable Energy, Vol. 31, PP. 317-331.
- Dippey, D.F and Saberskey, R.H.1963, Heat and momentum transfer in smooth and rough tubes at various Prandtl number. International Journal of Heat and Mass Transfer, Vol. 6, PP.239-253.
- Eiamsa- Ard, S. and Promvonge, P. 2008, Numerical study on heat transfer of turbulent channel flow over periodic grooves., International Journal of Heat Mass Transfer, Vol. 35, PP. 844-852.
- Forson, F. K., Nazha, M. A., Rajakaruna, H. 2003, Experimental simulation studies on a single pass double duct solar heater .Energy Conversion and Management, Vol. 44 , PP. 1209-1227.
- Gupta, I, Solnk, S.C and Saaini, J.S 1997, Thermohydrolic performance of solar air heaters with roughened absorber plate. Solar Energy, Vol. 61, No. 1, PP.33-42.
- Gupta,I, Solauki, S.C. and Saini, J.S 1997, Heat and fluid flow in asymmetricly roughed rectangular duct in transitionally rough flow, International Journal of Heat and Mass Transfer, Vol.19, PP.159-166.
- Han, J.C, Glicksman L.R, and Rosenow W.M. 1978, Investigation of heat transfer and friction for rib roughed surfaces. International Journal of Heat and MassTransfer, Vol. 21, PP.1143-1156.
- Han, J.C, Zhang, Y.M. and Lee, C.P. 1991, Augmented heat transfer is square channels with parallel crossed and V-shaped angled ribs. International Journal of Heat Transfer, Vol. 113, PP. 590-526.
- Momin, A. M. E, Saini, J.S., and Solanki, S.C. 2002, Heat transfer and friction in solar air heater duct with V-shaped rib roughness on absorber plate, International Journal of Heat and Mass Transfer Vol.45, No.16, PP. 3383-3396.
- Nguyen-chi, and Groll, M. 1982, Entrainment of flooding limit in a closed two-phase thermosyphon. Proc. 4th International Conference heat pipe, London UK, PP. 147-162.
- Prasad, B.N. and Saini, J.S 1998, Effect of artificial roughness on heat transfer and friction factor in solar air heater.Solar Energy, Vol.41, No. 6, PP.555-560.
- Promvonge, P. and Thianponge, C. 2008, Thermal performance assessment of turbulent channel flow over different shape ribs, International Commun heat mass transfer, Vol. 35, No.10, PP. 1327-1334.



- Skullong, S. 2017, Performance enhancement in solar air heater duct with inclined rib, mounted on the absorber., Journal of Research and Applications in mechanical engineering, Vol. 5, No.1, PP. 55-64.
- Sanjay, K. Shama, Vilas, R. Kalamkar, 2017, Experiment and numerical investigation of forced convective heat transfer in solar air heater with thin ribs. Solar Energy, Vol. 147, PP. 277-291.

Tatsumi, K., Iwai, H., Inooka, K., and Suzuki, K. 2003, Numerical analysis for heat transfer characteristics of an oblique discrete rib mounted in a square duct. Numerical Heat transfer, part A: Applications.

6. NOMENCLATURE

A	surface area of the collector plate, m^2 .
D_h	hydraulic mean diameter, m.
F_A	inclination angle factor.
H	height of the tunnel in the solar collector.
h_{cal}	calculated convective heat transfer coefficient, $W/m^2\text{ }^\circ\text{C}$.
h_{corr}	correlated convective heat transfer coefficient, $W/m^2\text{ }^\circ\text{C}$.
K_{air}	thermal conductivity of the air, $W/m\text{ }^\circ\text{C}$.
Nu	Nusselt number.
$N_{u_{corr}}$	correlated Nusselt number of air passage, m .
Q_u	useful heat gain carried away by the air per unit time, W.
\dot{m}	air mass flow rate, kg/s.
Re	Reynolds number.
T_{fi}	air temperature at inlet to the collector, $^\circ\text{C}$.
T_{fm}	average air temperature in the solar air heater, $^\circ\text{C}$.
T_{fo}	air temperature at the exit of the collector, $^\circ\text{C}$.
T_{pm}	average plate temperature, $^\circ\text{C}$.
V	velocity, m/s.
W	width of the tunnel in the solar collector of air passage, m.
α	inclination angle of the collector, Degree.
η_{ins}	instantaneous efficiency.
ν	kinematic viscosity of air, m^2/s .
ρ	Density of the air, kg/m^3 .

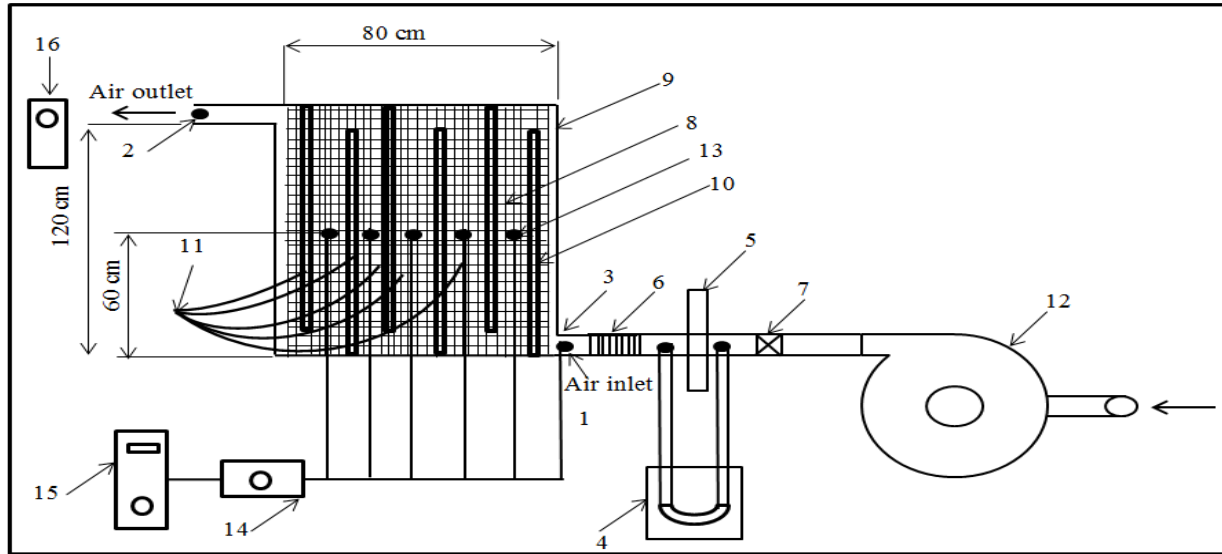


Figure 1a.Schematic diagram of the experimental setup.

(1-Entry point to collector ,2-Exit point.,3-Pipe (connecting pipe),.4-U-tube manometer.,5-Orifice.,6-Flexible pipe.,7-Control valve.,8-Wire mesh absorber.,9-Collector.,10-Plate (internal recycle plate),. 11-Air passage.,12-Blower unit.,13-Thermocouple junction (to measure local plate temperature),. 14-Selector switch.,15-Digital thermometer.,16-Digitalratometer.)

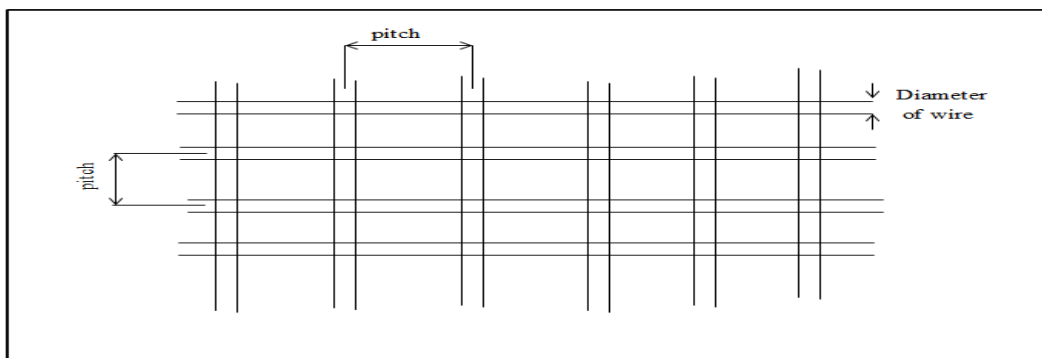


Figure 1b.Schematic of wire screen used as roughness element on absorber plate.
(wire diameter 0.5mm , pitch 1mm , porosity 0.958 , hydraulic radius 2.05×10^{-3} m)

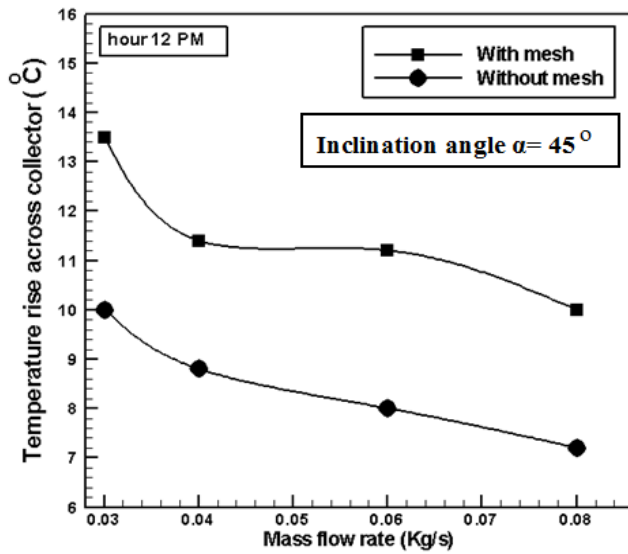


Figure 2. The effect of air mass flow rate on the temperature rise across the collector for various collector types.

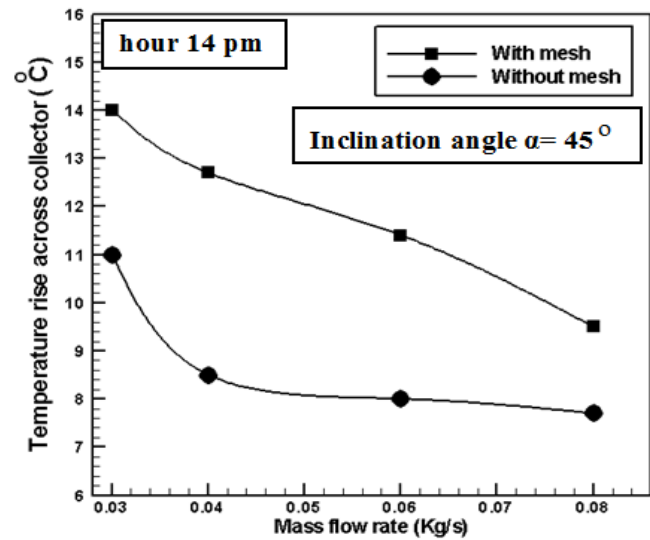


Figure 3. The effect of air mass flow rate on the temperature rise across the collector for various collector types.

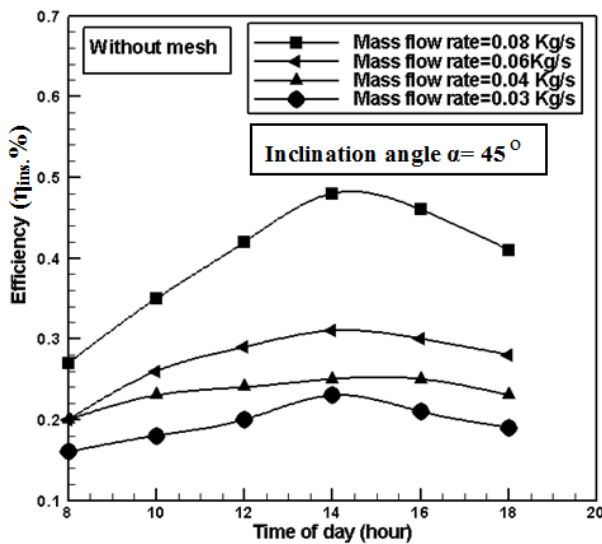


Figure 4. The variation of the instantaneous efficiency for various air mass flow rate.

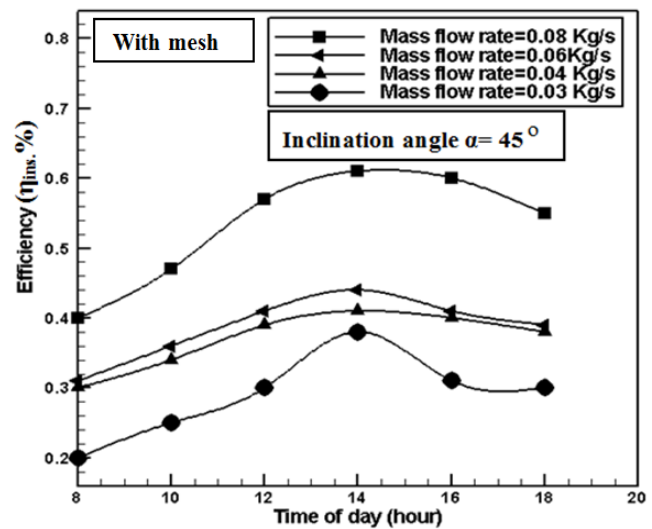


Figure 5. The variation of the instantaneous efficiency for various air mass flow rate.

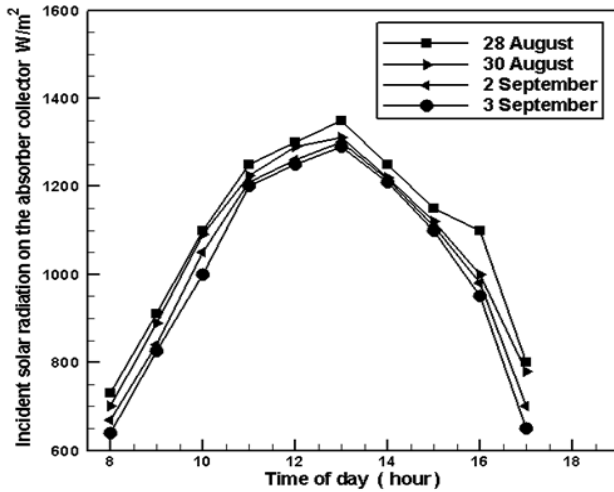


Figure 6. Incident solar radiation on the absorber as a function of day time for four days.

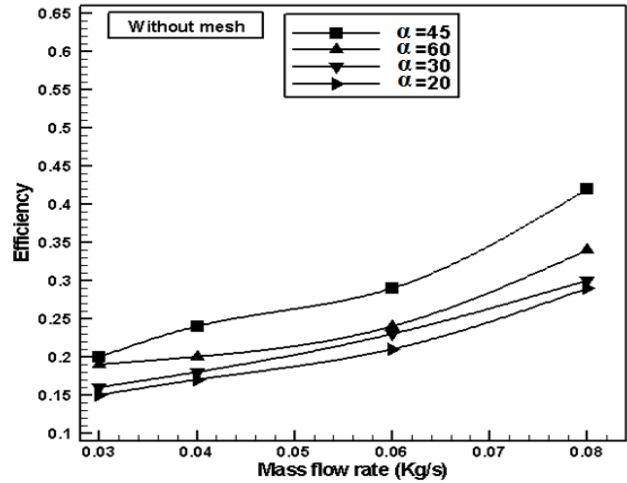


Figure 7. Instantaneous collector efficiency as a function of air mass flow rate for various inclination angles.

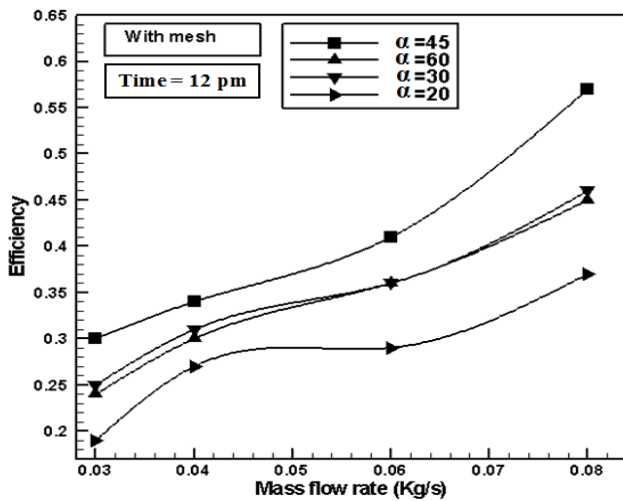


Figure 8. Instantaneous collector efficiency as a function of air mass flow rate for various inclination angles.

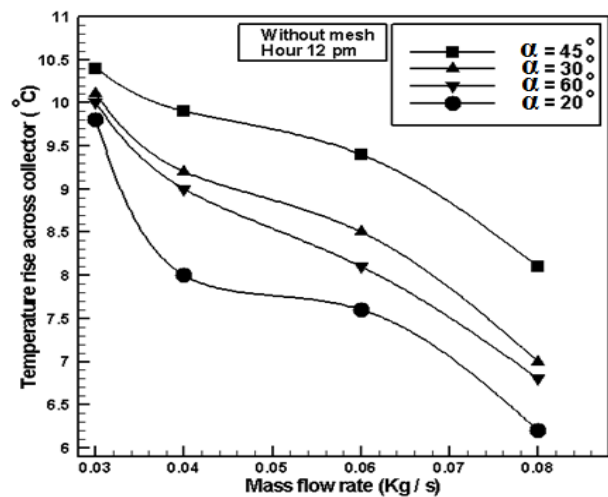


Figure 9. The variation of temperature rise across the collector with air mass flow rate for various inclination angles.

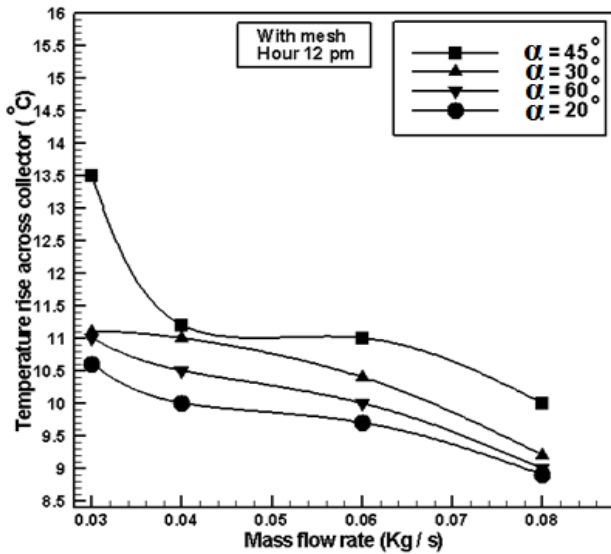


Figure 10. The variation of temperature rise across the collector with air mass flow rate for various inclination angles.

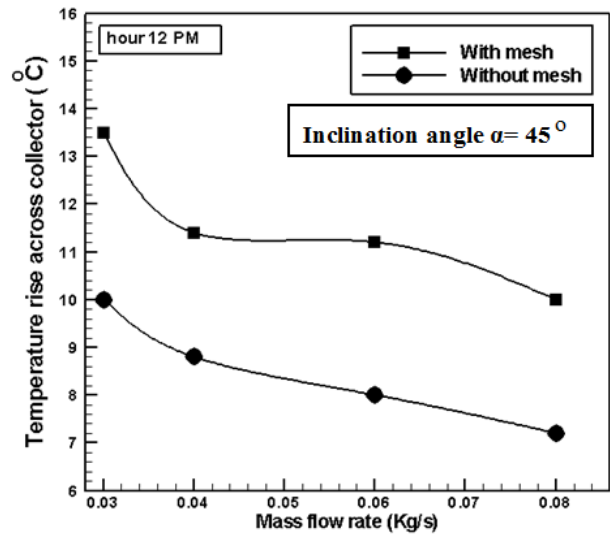


Figure 11. The variation of temperature rise across the collector with air mass flow rate With and without wire mesh.

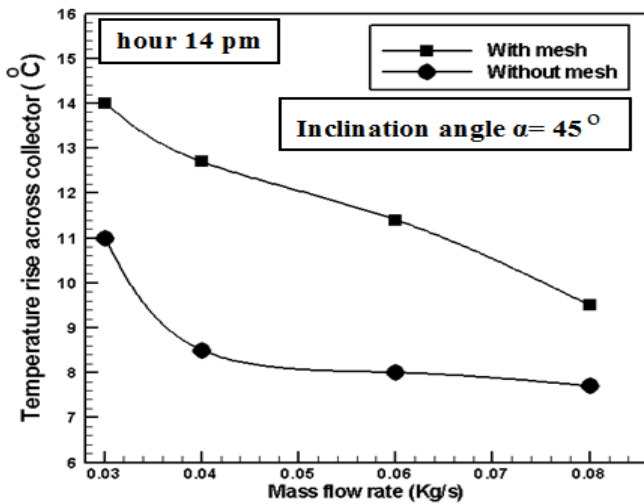


Figure 12. The variation of temperature rise across the collector with air mass flow rate with and without wire mesh.

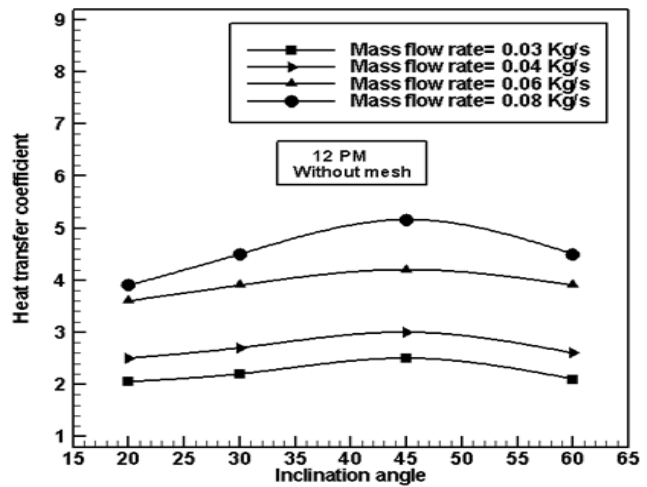


Figure 13. The variation of heat transfer coefficient with collector inclination angle For various air mass flow rate.

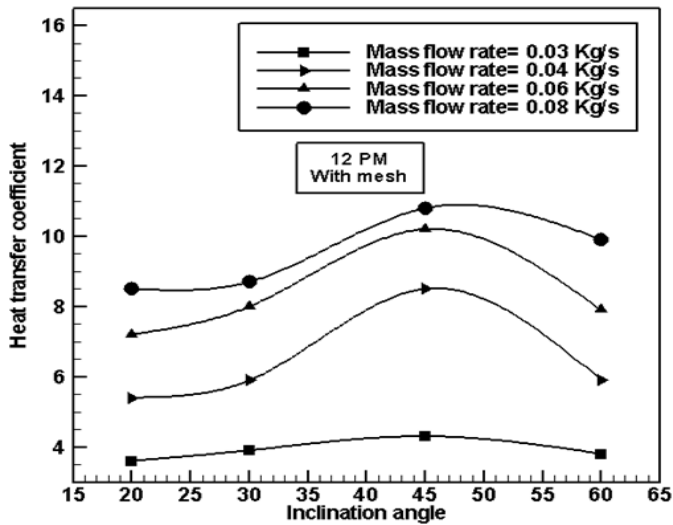


Figure 14. Heat transfer coefficient versus time of day for different mass flow rate of air.

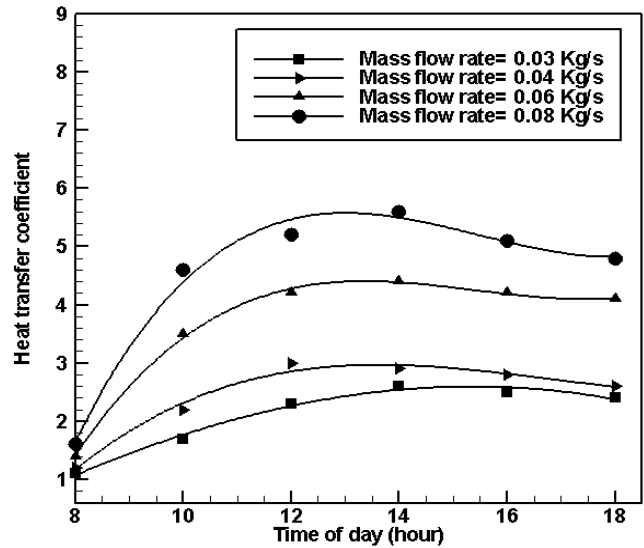


Figure 15. Heat transfer coefficient versus time of day for different mass flow rate of air.

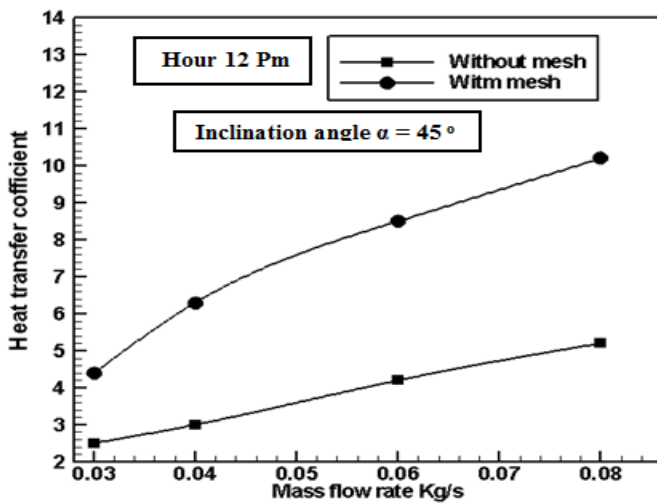


Figure 16. The variation of heat transfer coefficient with air mass flow rate with and without wire mesh.

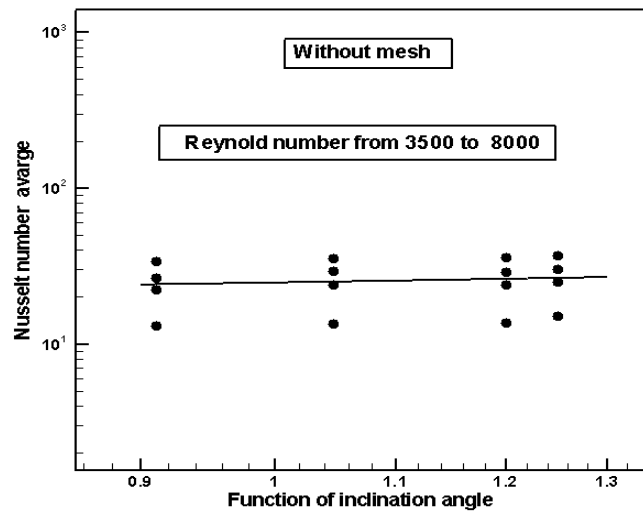


Figure 17. Relation between Nusselt number and the function of inclination angle.

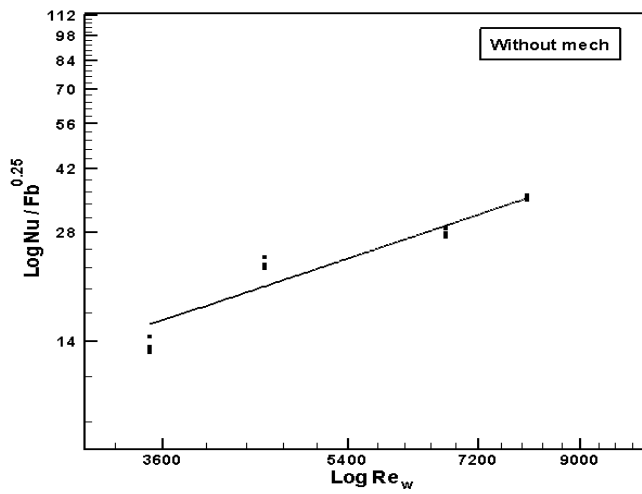


Figure 18. Data correlation for collector without wire mesh.

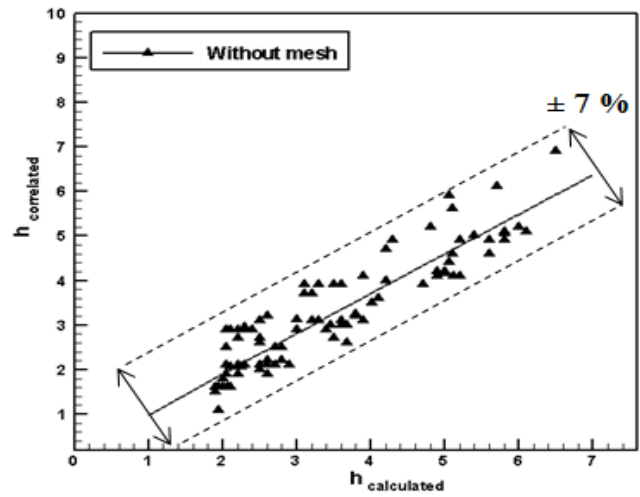


Figure 19. Comparison between calculated heat transfer coefficients with correlation heat transfer coefficient for the collector type without wire mesh.

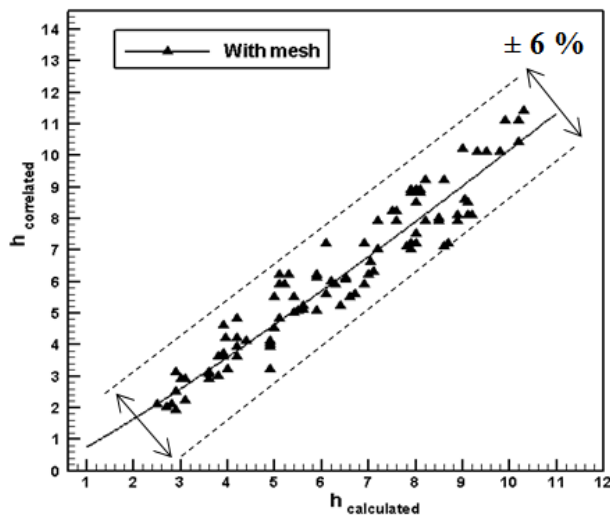


Figure 20. Comparison between calculated heat transfer coefficients with correlation heat transfer coefficient for the collector type with wire mesh.